SCIENCE CHINA
Technological Sciences

• Article •

September 2014 Vol.57 No.9: 1840–1845
doi: 10.1007/s11431-014-5553-x

Minimum detectable activity for NaI(Tl) airborne γ-ray spectrometry based on Monte Carlo simulation

GONG ChunHui[1,2], ZENG GuoQiang[2*], GE LiangQuan[2], TANG Xiaobin[1] & TAN ChengJun[2]

[1] *Department of Nuclear Science and Engineering, Nanjing University of Aeronautics and Astronautics, Nanjing 210016, China;*
[2] *College of Nuclear Technology and Automation Engineering, Chengdu University of Technology, Chengdu 610059, China*

Received December 3, 2013; accepted March 3, 2014

The determination of the effective minimum detectable activity (MDA) of radionuclides by a detection system plays an important role in environmental radiation monitoring. In this study, the responses of an NaI(Tl) airborne γ ray spectrometry (AGRS) system to different radionuclides (^{137}Cs and ^{131}I) were investigated using the Monte Carlo technique. The MDA values were determined under different conditions according to the counting spectra obtained from the Monte Carlo simulation. The equivalent mass thickness method was applied to the Monte Carlo modeling for monitoring ground radiation to reduce statistical uncertainty. The secondary source method was used to monitor both air and ground radiation. A quadratic relationship was found between the MDA and activity concentration. An exponential relationship was found between the MDA and altitude. The MDA of a specific radionuclide from external detectors was found to be superior to that obtained from internal detectors under the same conditions. The MDA values in an NaI(Tl) AGRS system under different conditions can be estimated based on the results of this study.

NaI(Tl) airborne γ ray spectrometry, minimum detectable activity, Monte Carlo simulation

Citation: Gong C H, Zeng G Q, Ge L Q, et al. Minimum detectable activity for NaI(Tl) airborne γ-ray spectrometry based on Monte Carlo simulation. Sci China Tech Sci, 2014, 57: 1840–1845, doi: 10.1007/s11431-014-5553-x

1 Introduction

For several decades, airborne γ ray spectrometry (AGRS) systems, which are composed of NaI(Tl) detectors mounted on an aircraft, have been widely used to record natural radiation intensity caused by potassium, uranium, and thorium through flying measurement for the purpose of mineral exploration and geological [1,2]. Given wide application of nuclear technology and the development of nuclear power, radiation protection has become an increasingly important topic. However, only a few studies have reported the use of AGRS to detect environmental contamination. Furthermore, these studies are generally concerned with determining the extent of contamination following nuclear accidents or locating strong artificial sources [2]. Unlike potassium, uranium, and thorium, radionuclides leaked in nuclear accidents, such as the most likely emitted radionuclides ^{131}I (0.364 MeV) and ^{137}Cs (0.662 MeV), emit low-power γ rays. As a result, detecting low-energy rays in the environment is less efficient.

A major problem in measuring radioactivity is determining detection efficiency and the minimum detectable activity (MDA) used to estimate the smallest amount of radionuclide activity that can be determined reliably [3]. Many methods have been used to determine the MDA or detection limit. However, experimentally determining detection efficiency in the environment for all γ ray energies is difficult because of limited number of single-energy, γ-emitting ra-

*Corresponding author (email: zgq@cdut.edu.cn)

dionuclides distributed in the air and ground.

Monte Carlo simulations are the gold standard in the study of radiation dosimetry, detector design, and so on. Open environment efficiency calibration and study of the MDA of AGRS using the Monte Carlo technique are still pending. In the present work, we determine the detection efficiency for each type of γ ray energy by performing a Monte Carlo simulation using the MCNP5 [4] code to calculate the detection efficiency of different radionuclides in the air and ground environment. Using the simulated efficiency, MDA is also calculated using the Currie method [5] for different radionuclides and different circumstances.

2 Theoretical basis and simulations

2.1 MDA estimation

MDA can be calculated for radionuclides that are found and unfound in the spectrum [6]. Various methods for determining MDA have been developed; the methods developed by Currie are widely accepted and used as basis [5]. The MDA in becquerels per square meter (or cubic meter) is calculated using eq. (1):

$$\mathrm{MDA} = \frac{L_D}{\varepsilon_m \cdot p \cdot T_l}, \tag{1}$$

where T_l is the collection time (in seconds), p is the emission probability, and ε_m is the detection efficiency in m^2 or m^3 as calculated using eq. (2), respectively.

$$\begin{aligned} \varepsilon_m &= \varepsilon \cdot V, \\ \varepsilon_m &= \varepsilon \cdot S, \end{aligned} \tag{2}$$

where ε is the photopeak efficiency at a specific energy, V is the volume of air for each γ ray (in m^3), and S is the area of areal source for each γ ray (in m^2).

According to the definitions for critical level (L_C) and detection limit (L_D),

$$L_C = k_\alpha \sigma_0, \tag{3}$$

$$L_D = L_C + k_\beta \sigma_D = L_C + k_\beta \sqrt{L_D + \sigma_0^2}, \tag{4}$$

and setting $k_\alpha = k_\beta = k$,

$$\begin{aligned} L_D &= k^2 + 2L_C = k^2 + 2k\sqrt{(B + \sigma^2(B))} \\ &= 2.71 + 3.29\sqrt{(B + \sigma^2(B))}, \end{aligned} \tag{5}$$

where k_α and k_β are abscissas of the standardized normal distribution corresponding to probability levels 1-α and 1-β, respectively; σ_0 and σ_D are the standard deviations of the net signal when the true net signal is null and when the true net signal is equal to the detection limit, respectively; B is the number of background baseline counts under the γ ray peak in the region of interest (ROI); and $\sigma^2(B)$ is the variance of B. For a probability equal to 0.05, k is 1.645.

For a linear continuum background, B is given by eq. (6).

$$B = (B_1 + B_2)N/(2m), \tag{6}$$

where B_1 and B_2 are the sums of counts in the m channels to the left and in the m channels to the right of the ROI, respectively; N is the number of channels in the ROI (Figure 1). In the present work, m was set to 1.

For a peak found in the spectrum, B_1 and B_2 are independent and normally distributed [7], and the variance of B can be given by eq. (7).

$$\sigma^2(B) = BN/(2m). \tag{7}$$

2.2 Simulation setup

The GRS-16 system (Pico Envirotec Inc., Canada) is an intelligent, self-calibrating γ ray spectrometer that uses NaI(Tl) large-volume detector arrays. GRS-16 is used in natural and artificial radiation contamination detection. The NaI(Tl) airborne γ ray spectrometer uses a total of 10 to 20 sodium iodide thallium-activated NaI(Tl) crystals, which are fabricated as long-type detectors with dimensions of 4″ × 4″ × 16″. The most number of crystals used is 15, as shown in Figure 2. These detectors are packaged in three units. Each unit is a 2 mm aluminum box containing five crystals with four lying parallel at the bottom and one lying at the center of the top. Each crystal is wrapped with 2 mm permalloy [7].

We used the general-purpose Monte Carlo N-Particle code MCNP5 to perform the simulation. The geometry was fully modeled according to the description shown in Figure 2. The elemental compositions of the materials used in the simulation are listed in Table 1.

The F8 pulse-height tally was used to obtain the pulse height per emitted particle in the source, i.e., absolute efficiency for each spectrum peak in the source and for each modeled geometry. The Gaussian Energy Broadening card was used to obtain an improved simulation of the whole

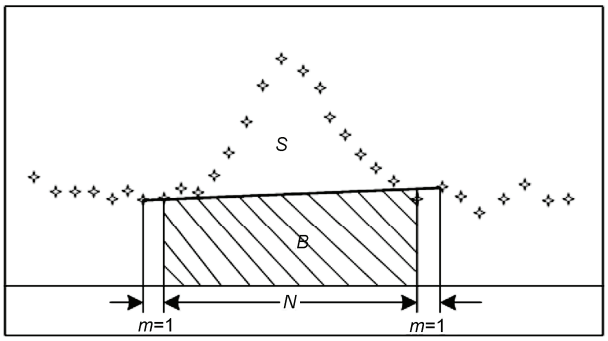

Figure 1 Parameters used in a step function continuum calculation of the peak area.

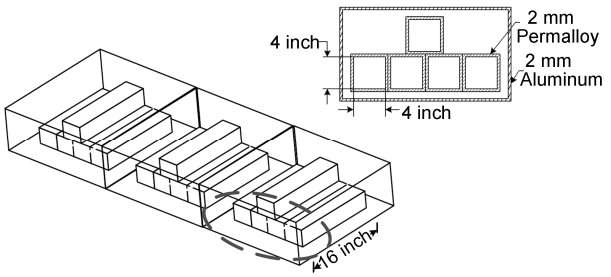

Figure 2 GRS-16 boxes with 4″ × 4″ × 16″ sodium iodide thallium-activated NaI(Tl) crystals.

Table 1 Composition of material in the detector

Material	Composition (atomic ratio)	Density (g/cm^3)
Air	N (75.611%), O (23.186%), Ar (1.157%), C (0.045%), H (0.001%)	1.293×10^{-3}
Aluminum box	Al (100%)	2.7
Crystal shell (permalloy)	Ni (80%), Mo (4.4%), Si (0.3%), Mn (0.5%), Fe (14.8%)	8.74
NaI(Tl) crystal	Na (49.9%), I (49.9%), Tl (0.2%)	3.67

spectrum. This card broadens the γ ray peaks based on the energy-dependent eq. (8). The values of a, b, and c were algebraically solved using the measured full width at half maximum (FWHM) values of 36.89, 37.65, 52.46, 23.55, 30.73, and 43.03 keV and the corresponding γ ray energy values of 2626, 1460, 946, 600.2, 352, and 253.9 keV. The results were obtained: $a = 0.0282$, $b = 0.0135$, $c = -0.3186$.

$$\mathrm{FWHM} = a + b\sqrt{E + cE^2}, \tag{8}$$

where FWHM is the full width of the γ ray peak at half its maximum value, E is the energy of the γ ray peak (MeV), a is independent parameter 1 (MeV), b is independent parameter 2 (MeV$^{1/2}$), and c is independent parameter 3 (none).

In actual aerial surveys, the γ ray spectrometer is usually mounted on an aircraft. Compared with external detectors, internal detectors have lower detection efficiency because low-energy γ rays are seriously attenuated by the shielding of the aircraft shell. In the present work, we discuss the MDA difference between internal and external detectors.

3 MDAs in monitoring air radiation

To simulate actual air radiation monitoring conditions, a sphere volumetric source was used to simulate a radioactive plume. The required radius R, covered by γ rays in the air to reduce their density I to 0.1% of its initial value I_0, depends on the energy. To monitor air radiation, a spherical volume V_{eff} surrounding the detector was defined as the "effective volume" for the specific γ ray energy; beyond this sphere, γ rays have practically zero probability of reaching and interacting with the detector crystal [8]. R can be calculated from the total attenuation coefficient $\mu(E)$ using eq. (9).

$$\left.\begin{aligned} I &= I_0 \mathrm{e}^{-u(E)R} \\ I &= 0.001 I_0 \end{aligned}\right\} \Rightarrow R(m) = \frac{6.91}{u(E)}. \tag{9}$$

In the present work,

$$\begin{aligned} R &= \frac{6.91}{u(E)} = \frac{6.91}{5.504\times10^{-3}\ \mathrm{m^2/kg}\times 1.293\ \mathrm{kg/m^3}} \\ &= 971\ \mathrm{m}. \end{aligned} \tag{10}$$

Therefore, the NaI(Tl) AGRS system was covered by 1 km of air, which was enough to simulate a realistic environment for energies $E\gamma < 1.33$ MeV; the altitude of the aircraft was H (Figure 3). The aerial survey altitude ranged from 80 m to 200 m [9].

The isotropical source was uniformly distributed across a very large volume. The AGRS was rather small relative to the source. A secondary source was set to reduce the variance in the simulation results in the present work. A sphere with a 5 m radius around the detectors was set to record the fluence and energy spectrum of the particles into the sphere in MCNP5. A sphere surface source with this fluence and spectrum was set as Source 1. In addition, a volumetric source surrounding the detector with a radius of 5 m was set as Source 2. The pulse height distributions were then calculated using Sources 1 and 2. Finally, the total pulse height distribution was obtained by summing up these two pulse height distributions proportionally.

MDA estimation is based on one overflight with a known background count rate level. Furthermore, the background count rate varies from one point to another. In the present work, different activity concentrations and multiple heights were simulated. The detection efficiency and background count rate for specific radiation sources were obtained using MCNP5. The MDAs of the external detectors at 80 m for ^{137}Cs at different activity concentrations as shown in Table 2. The relationship (Figure 4) between MDA and activity concentration is expressed as eq. (11).

$$\mathrm{MDA} = -1.05804\mathrm{e}^{-5}x^2 + 0.0026x + 0.05114, \tag{11}$$

where x is the activity concentration. This equation exactly follows the MDA algorithm in eq. (1). MDA is related to the background quadratically, which is determined by the activity concentration.

The pulse height distribution spectra of the external and internal detectors clearly differ, as shown in Figure 5. The external relative counts are larger than the internal relative counts given the same measurement conditions.

The MDAs of the external and internal detectors are different under the same conditions, as shown in Table 3. Table 3 shows that the MDAs of the external and internal detectors have different altitudes for two radionuclides (^{137}Cs, ^{131}I). The MDA value of the external detectors at the same height is lower than the MDA value of the internal detectors. This result implies that the external detectors are superior to the internal detectors.

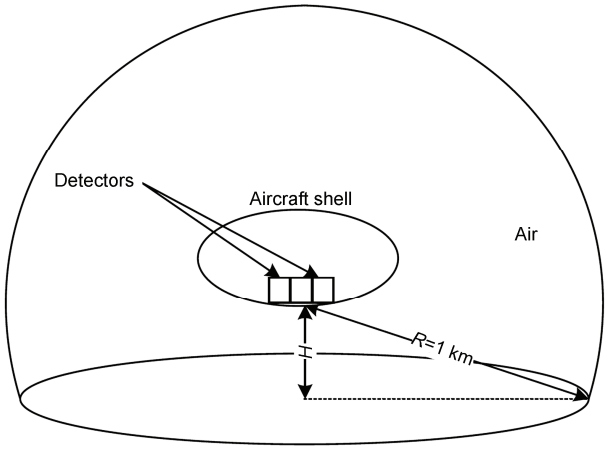

Figure 3 Monitoring air radiation.

Table 2 MDAs for ^{137}Cs at different activity concentrations at 80 m using external detectors

Activity Concentration (kBq/m^3)	MDA (kBq/m^3) a)	Activity Concentration (kBq/m^3)	MDA (kBq/m^3) a)
23	0.105	43	0.143
25	0.109	45	0.147
27	0.114	47	0.150
29	0.118	49	0.153
31	0.122	51	0.156
33	0.126	53	0.159
35	0.129	55	0.162
37	0.133	57	0.165
39	0.137	59	0.168
41	0.140	61	0.171

a) The collection time is 1 s.

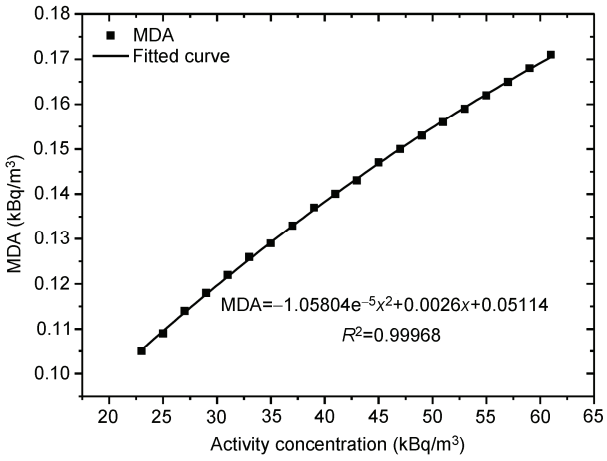

Figure 4 Graphic representation of MDA values at the 0.662 MeV photopeak of the simulated spectrum at different activity concentrations.

4 MDAs in monitoring ground radiation

As described in the previous section, an aircraft was set to record the fluence and energy spectrum of the particles across the aircraft from the bottom. These particles were used as the secondary source to simulate the pulse height distribution in the detector.

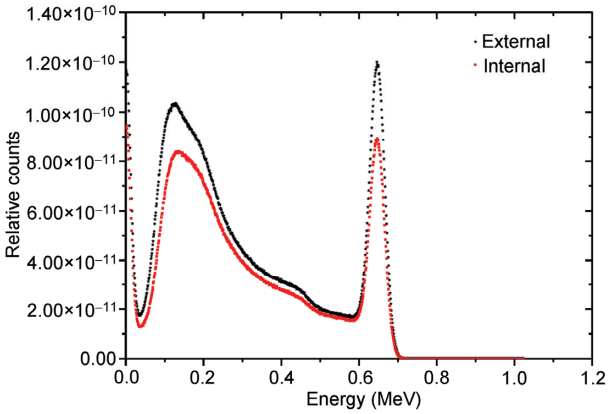

Figure 5 (Color online) The MCNP pulse height output spectra of external and internal detectors at a height of 80 m.

Moreover, equivalent mass thickness was used in this study, i.e., air density was changed under the same thickness to simulate different altitudes. The principle underlying this variation indicates that the unscattered photon flux at a certain point will be the same when particles pass through the same mass thickness in the medium. We verify this theory using the following method.

The monitoring of ground radiation is depicted in Figure 6, where r denotes the source radius, h denotes the linear distance from the ground to the aircraft bottom, and R denotes the slope distance from the ground to the aircraft bottom.

Here, we set μ as the linear attenuation coefficient of the media to γ photon at a specific energy, (μ/ρ) as the mass attenuation coefficient of the media to γ photon, and Φ as the unscattered photon flux. r_1, h_1, R_1, μ_1, and Φ_1 are used in

Table 3 MDAs for two radionuclides at different altitudes as calculated from their most intense γ rays (in MeV) using external and internal detectors.

Altitude(m)	MDA (kBq/m^3) a)			
	^{137}Cs (0.662 MeV)		^{131}I (0.364 MeV)	
	External	Internal	External	Internal
80	0.120	0.138	0.143	0.173
90	0.118	0.137	0.141	0.171
100	0.118	0.136	0.140	0.171
110	0.117	0.136	0.140	0.169
120	0.117	0.135	0.139	0.169
130	0.115	0.134	0.139	0.168
140	0.116	0.133	0.139	0.168
150	0.116	0.132	0.138	0.167
160	0.116	0.133	0.138	0.167
170	0.115	0.133	0.138	0.167
180	0.116	0.132	0.138	0.168
190	0.115	0.133	0.137	0.167
200	0.115	0.133	0.138	0.167

a) The collection time is 1 s, and the activity concentration is 30 kBq/m^3.

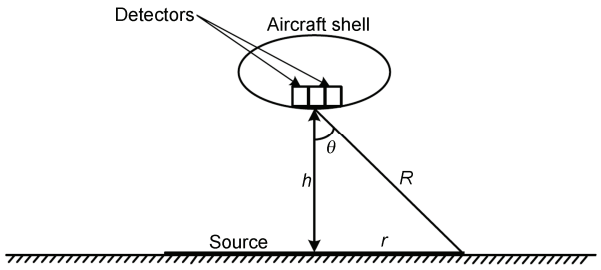

Figure 6 Monitoring ground radiation.

the simulation, whereas r_2, h_2, R_2, μ_2, and Φ_2 are used in the actual measurement.

$$\Phi_1 = A_S \int \frac{1}{4\pi R_1^2} \mathrm{e}^{-\mu_1 R_1} \cdot 2\pi r_1 \mathrm{d}r_1, \tag{12}$$

$$R_1 = h_1 \sec\theta, \tag{13}$$

$$r_1 = h_1 \tan\theta \Rightarrow \mathrm{d}r_1 = h_1 \sec^2\theta \mathrm{d}\theta, \tag{14}$$

$$\Rightarrow \Phi_1 = A_S \int \frac{\mathrm{e}^{-\mu_1 h_1 \sec\theta}}{4\pi h_1^2 \sec^2\theta} \cdot 2\pi h_1 \tan\theta \cdot h_1 \sec^2\theta \mathrm{d}\theta$$

$$= A_S \int \frac{\tan\theta \cdot e^{-\mu_1 h_1 \sec\theta}}{2} \mathrm{d}\theta. \tag{15}$$

Similarly,

$$\Phi_2 = A_S \int \frac{\tan\theta \cdot \mathrm{e}^{-\mu_2 h_2 \sec\theta}}{2} \mathrm{d}\theta. \tag{16}$$

We assume that the mass thickness is constant in theory, namely,

$$\rho_1 h_1 = \rho_2 h_2, \tag{17}$$

$$\Rightarrow \frac{h_1}{h_2} = \frac{\rho_2}{\rho_1} = \frac{(\mu_2/\rho_2)\cdot\rho_2}{(\mu_1/\rho_1)\cdot\rho_1} = \frac{\mu_2}{\mu_1}, \tag{18}$$

$$\Rightarrow \mu_1 h_1 = \mu_2 h_2, \tag{19}$$

$$\Rightarrow A_S \int \frac{\tan\theta \cdot \mathrm{e}^{-\mu_1 h_1 \sec\theta}}{2} \mathrm{d}\theta = A_S \int \frac{\tan\theta \cdot \mathrm{e}^{-\mu_2 h_2 \sec\theta}}{2} \mathrm{d}\theta, \tag{20}$$

$$\Rightarrow \Phi_1 = \Phi_2. \tag{21}$$

According to eq. (10), the "effective area" with a radius R is defined for different altitudes, i.e., the radius of the source was set to 965 m for monitoring ground radiation, the altitude was set to 100 m, and so forth. The activity concentration of ^{137}Cs that leaked from the Chernobyl accident ranged from 23 kBq/m^2 to 185 kBq/m^2 [10,11]. The MDAs of the internal detectors at 80 m for ^{137}Cs with different activity concentrations are given in Table 4. The MDA for ^{137}Cs was improved by reducing the activity concentration. The detected minimum activity concentration at the altitude of 80 m was 45 kBq/m^2 in the simulation.

The relationship between MDA and activity concentration is shown in Figure 7. The fitted curve formula is given by eq. (22).

$$\mathrm{MDA} = -0.00367x^2 + 0.82404x + 15.01684, \tag{22}$$

where x is the activity concentration. eq. (22) shows that MDA is related to the background quadratically, which is determined using the activity concentration.

The MDAs of the external and internal detectors are different given the same conditions, as shown in Table 5. Table 5 shows the MDAs of the external and internal detectors at different altitudes for two radionuclides (^{137}Cs, ^{131}I). MDA increases as altitude increases.

The external detectors to ^{137}Cs at different altitudes follow the discipline given in eq. (23).

$$\mathrm{MDA} = -35.25903 + 53.09377\mathrm{e}^{x/191.34811}. \tag{23}$$

Similarly, the internal detectors to ^{137}Cs follow the discipline given in eq. (24).

$$\mathrm{MDA} = -28.28135 + 50.93232\mathrm{e}^{x/178.65585}, \tag{24}$$

where x represents the altitude. It can be attributed to the exponential γ ray attenuation in the medium that exponentially reduces the detection efficiency as the altitude increases. An exponential relationship therefore exists between MDA values and altitude. Figure 8 shows that the external detectors are superior to the internal detectors. The MDA of the external detectors at a height of 100 m is nearly equal to that of the internal detectors at a height of 90 m. Considering the actual aerial survey in which the minimum flying height of the fixed-wing plan is only 100 m, the external detectors is regarded as the best method for monitoring ground radiation.

5 Conclusion

In the present study, an NaI(Tl) AGRS used in radiation environmental monitoring was simulated to estimate effective MDA values when measuring the γ ray at various altitudes. This study provides a basis for obtaining an effective measurement of environmental radioactivity.

Table 4 MDAs for ^{137}Cs with different activity concentrations at 80 m as calculated from the most intense γ rays (in MeV) using internal detectors

Activity Concentration (kBq/m^2)	MDA (kBq/m^2) a)	Activity Concentration (kBq/m^2)	MDA (kBq/m^2) a)
23	31.962	49	46.563
25	33.314	51	47.500
27	34.613	53	48.418
29	35.866	55	49.320
31	37.075	60	51.504
33	38.246	65	53.600
35	39.382	70	55.615
37	40.487	75	57.561
39	41.516	80	59.442
41	42.609	85	61.266
43	43.631	90	63.036
45	44.630	95	64.758
47	45.630	100	66.436

a) The collection time is 1 s.

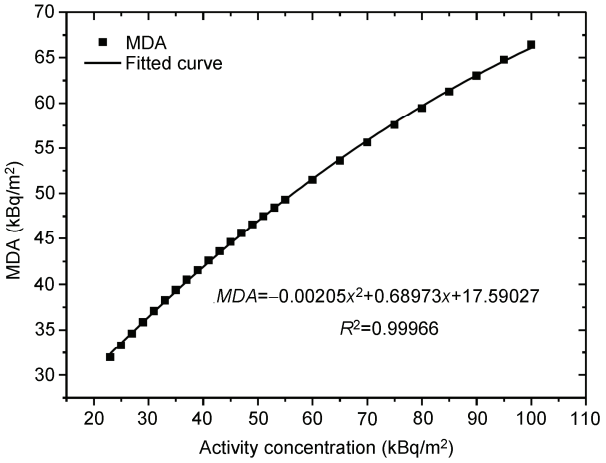

Figure 7 Graphic representation of MDA values at the 0.662 MeV photopeak of the simulated spectrum at different activity concentrations.

Table 5 MDAs for two radionuclides at different altitudes as calculated from their most intense γ rays (in MeV) using external and internal detectors.

Altitude (m)	MDA (kBq/m^2) [a]			
	^{137}Cs (0.662 MeV)		^{131}I (0.364 MeV)	
	External	Internal	External	Internal
80	45.423	51.504	74.002	82.523
90	49.652	55.910	81.488	90.710
100	54.349	60.925	89.965	99.711
110	59.185	66.090	98.471	109.278
120	64.076	71.322	107.329	118.933
130	69.379	77.066	117.291	129.527
140	74.917	83.067	127.943	140.974
150	81.137	89.561	139.259	153.577
160	87.309	96.712	150.056	165.771
170	93.961	103.716	162.898	179.595
180	100.741	111.338	176.170	193.866
190	107.974	119.045	190.025	208.954

a) The collection time is 1 s, and the activity concentrations for ^{137}Cs and ^{131}I are 60 kBq/m^2 and 100 kBq/m^2, respectively.

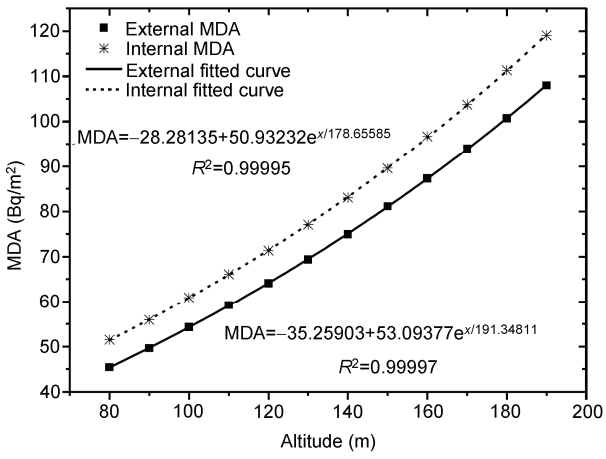

Figure 8 Graphic representation of MDA values at the 0.662 MeV photopeak of the simulated spectrum at different altitudes.

To reduce the variance of the simulation result, the equivalent mass thickness method was used for the Monte Carlo simulation of ground radiation monitoring. The secondary source method was used to monitor both air and ground radiations. The feasibility of simulating the AGRS to estimate the effective MDA values is demonstrated. Given that MDA is related to the activity concentration and the altitude of the detectors, a quadratic relationship was found between MDA and activity concentration for a radionuclide at the same altitude. Moreover, both MDA and altitude complied with the exponential law in monitoring ground radiation. According to the MDA value, external detectors can be adopted in overflight measurements instead of internal detectors to improve MDA.

However, this study has a number of limitations, including simulation conditions that are too idealistic. During the simulation of air radiation monitoring, we simplified the radioactive plume using a sphere volumetric source, wherein the radiation plume is composed of radioactive materials scattering like smoke in the wind. We did not consider the air radiation existing alongside the ground radiation. Instead of measuring the background, we used the product of the simulated count rate and activity as the background count to estimate MDA. Following the conclusion of the present study, we plan to compare the different results using different detector setups in different environments to find the appropriate solution for environmental radiation monitoring.

This work was supported by the National Defense Basic Scientific Research Project (Grant No. B2520133077), and National High-tech R&D Program of China ("863" Program) (Grant No. 2012AA061803).

1 Bristow Q. Airborne γ-ray spectrometry in uranium exploration. Principles and current practice. Int J Appl Rad Isotop, 1983, 34: 199–229
2 Paul M, Stephen T, Anthony M, et al. Use of airborne γ-ray spectrometry for environmental assessment of the rehabilitated nabarlek uranium mine, australia. Environ Monitor Assess, 2006, 115: 531–554
3 Nir-El Y, Haquin G. Minimum detectable activity in in situ γ-ray spectrometry. Appl Rad Iso, 2001, 55: 197–203
4 X-5 Monte Carlo Team. MCNP-A general Monte Carlo N-particle transport code. Version 5, Los Alamos National Laboratory, Report LA-UR-03-1987, 2003
5 Currie L A. Limits for qualitative detection and quantitative determination. Anal Chem, 1986, 40: 586–593
6 Canberra. Genie™ 2000 Spectroscopy Software Customization Tools. 2006, 345–346
7 Zhang H R, Fan Z G. Recent advances in aerogeophysical techniques used abroad. Geophys Geochem Explor, 2007, 31: 1–8
8 Bagatelas C, Tsabaris C, Kokkoris M, et al. Determination of marine gamma activity and study of the minimum detectable activity (MDA) in 4pi geometry based on Monte Carlo simulation. Environ Monitor Assess, 2010, 165: 159–168
9 Jia M Y, Huang X L, Su X J, et al. Scale device of aerial radioactivity measuring system based on virtual source principle. CN 201732166 U, 2011
10 Roy Pöllänen, Harri Toivonen, Kari Peräjärvi, et al. Radiation surveillance using an unmanned aerial vehicle. Appl Rad Iso, 2009, 67: 340–344
11 Gu N G, Wu J H. Nuclear (Radiological) Emergency Disposal. Shanghai: Fudan University Press, 2004